FULL PAPER

Mechanochromic Luminescence (MCL) of Purely Organic Two-Component Dyes: Wide-Range MCL over 300 nm and Two-Step MCL by Charge-Transfer Complexation

Suguru Ito,*[a] Ryohei Sekine,[a] Masayasu Munakata,[a] Maho Yamashita,[b] and Takashi Tachikawa*[b,c]

[a] Prof. Dr. S. Ito, R. Sekine, M. Munakata
Department of Chemistry and Life Science, Graduate School of Engineering Science
Yokohama National University
79-5 Tokiwadai, Hodogaya-ku, Yokohama 240-8501 (Japan)
E-mail: suguru-ito@ynu.ac.jp

[b] M. Yamashita, Prof. Dr. T. Tachikawa
Department of Chemistry
Graduate School of Science, Kobe University
1-1 Rokkodai-cho, Nada-ku, Kobe 657-8501 (Japan)

[c] Prof. Dr. T. Tachikawa
Molecular Photoscience Research Center, Kobe University
1-1 Rokkodai-cho, Nada-ku, Kobe 657-8501 (Japan)
E-mail: tachikawa@port.kobe-u.ac.jp

Supporting information for this article is given via a link at the end of the document.

Abstract: Despite recent extensive studies on mechanochromic luminescence (MCL), rational control over the magnitude of the emission-wavelength shift in response to mechanical stimuli remains challenging. In the present study, a two-component donor–acceptor approach has been applied to create a variety of organic MCL composites that exhibit remarkable emission-wavelength switching. Dibenzofuran-based bis(1-pyrenylmethyl)diamine and typical organic fluorophores have been employed as donor and acceptor dyes, respectively. Outstanding wide-range MCL with an emission-wavelength shift of over 300 nm has been achieved by mixing the diamine with 3,4,9,10-perylenetetracarboxylic diimide. Unprecedented two-step MCL in response to mechanical stimuli of different intensity has also been realized for a two-component mixture with 9,10-anthraquinone. Fluorescence microscopy observations at the single-particle level revealed that the segregation and mixing of the two-component dyes contribute to the stimuli-responsive emission-color switching of the MCL composites.

Introduction

Solid-state reversible color switching of photoluminescence induced by a mechanical stimulus is referred to as mechanochromic luminescence (MCL). This phenomenon is attracting increasing attention on account of its diverse potential applications, including force sensors, rewritable data storage, and security inks.[1,2] The MCL of crystalline compounds is typically attributed to the alteration of the steric and electronic states of the luminescent molecules due to the amorphization of the crystal structure in response to a mechanical stimulus (Figure 1a). The original crystalline state can usually be recovered from the mechanically induced amorphous state by heating or exposure to solvents. From a practical perspective, purely organic MCL dyes have advantages in terms of processability and low toxicity. Moreover, it would be desirable that the emission spectra of the initial and mechanically altered states do not overlap. Although the majority of hitherto reported MCL dyes are purely organic compounds, the shifts in their maximum emission wavelengths are generally narrower than those of organometallic MCL dyes.[2l,3] Specifically, the MCL shift is less than 100 nm for most reported organic MCL dyes.[4] Obtaining wide-range MCL using purely organic fluorophores thus remains a challenging task.

Another emerging challenge in the development of organic MCL dyes is the realization of stepwise emission-color switching in response to mechanical stimuli of different intensity. This type of MCL dyes would be applicable to advanced detection systems for mechanical stimuli. Previous reports on stepwise MCL have involved the occasional discovery of crystalline dyes that exhibit successive emission-color changes upon gentle grinding followed by strong grinding.[5] The general mechanism of this typical two-step MCL has been based on a crystal-to-crystal transition upon gentle grinding followed by a crystal-to-amorphous transition upon strong grinding. Even though a ring-opening reaction induced by strong grinding has been shown to be an efficient trigger for the second emission-color change for some two-step MCL dyes,[6] detailed rational guidelines for the design of organic dyes with two-step MCL properties have not yet been established.

Herein, we report a two-component donor–acceptor strategy to rationally control the MCL shift. A useful approach to achieve wide-range MCL is the use of Förster resonance energy transfer (FRET) from the donor to the acceptor dye. Although a few two-component systems utilizing FRET to control the MCL shift of organic dyes have been reported, these previous examples require two organic MCL dyes.[6c,7] Recently, we have reported that the MCL shift of pyrenylthiophene derivatives can be tuned by mixing them with *N*,*N*′-dimethylquinacridone (**DMQA**), which does not exhibit MCL properties.[8] In the present study, a series of organic non-MCL dyes has been used as acceptor dyes to control the MCL properties of dibenzofuran-based bis(1-pyrenylmethyl)diamine **1** (Figure 1b). Most remarkably, a large MCL shift of over 300 nm was achieved by combining **1** with a far-red emissive organic dye. Single-particle-level observations using fluorescence microscopy revealed that the transition between

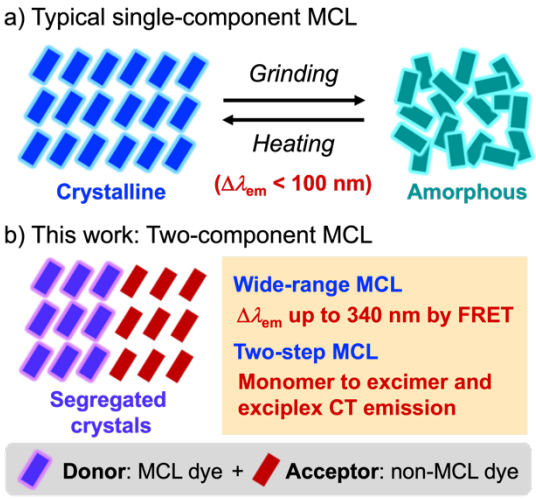

Figure 1. Schematic illustration of a) typical single-component MCL and b) the two-component MCL reported in this work.

segregated crystals and an amorphous mixture is responsible for the wide-range MCL of the two-component dyes based on the FRET mechanism. Furthermore, two-step MCL based on the mechanical-stimulus-induced formation of charge-transfer (CT) complexes has been achieved for the first time. In sharp contrast to the recently reported CT-based bicolor MCL systems,[9] the stepwise emission-color change in this work has been realized via the combination of monomer-to-excimer switching and excimer-to-exciplex switching.

Results and Discussion

Preparation and MCL properties of 1

During our study on dibenzofuran-based C_2-symmetric diamine derivatives,[10] dibenzofuran-based bis(1-pyrenylmethyl)diamine **1** was synthesized in five steps from the known precursor dibenzo[*b*,*d*]furan-4,6-diyldimethanol (**2**: Scheme 1).[11] The Mitsunobu azidation of **2** by treatment with triphenylphosphine, diisopropyl azodicarboxylate (DIAD), and diphenylphosphoryl azide (dppa) in THF at –20 °C for 26 h gave diazide **3** in 59% yield. The reduction of the azide groups of **3** in the presence of 5% palladium on carbon (Pd/C) under hydrogen atmosphere in ethyl acetate at room temperature for 21 h afforded diamine **4** in 77% yield. Nosyl (Ns: 2-nitrobenzenesulfonyl) groups were then introduced by the reaction of **4** with NsCl in the presence of Et_3N in THF at room temperature for 22 h to give **5** in 59% yield. Pyrenylmethylation of **5** was carried out by mixing **5** with 1-(bromomethyl)pyrene in the presence of K_2CO_3 in DMF at 60 °C for 1.5 h to afford **6** in 98% yield. The removal of Ns groups by the reaction of **6** with thiophenol and aqueous KOH solution in CH_3CN at 50 °C for 45 min afforded **1** in 74% yield.

Powdered samples of **1**, obtained by cooling a hot toluene solution of **1**, exhibited blue emission with a maximum emission wavelength (λ_{em}) of 433 nm (Figure 2a). The fluorescence quantum yield (Φ_F) of the blue emission was 0.05. Powder X-ray diffraction (PXRD) analysis showed that the powdered samples of **1** were aggregates of microcrystals (Figure 2c). Upon grinding with a spatula, the emission color of crystalline **1** changed to blue-green (λ_{em} = 487 nm, Φ_F = 0.30), and the mean fluorescence lifetime (<τ>) increased from 2.1 ns to 3.8 ns (Figure 2b and Table S1). The original blue emission color (λ_{em} = 427 nm) can be restored upon heating the ground sample to 150 °C on a hotplate. The grinding/heating process is fully reversible and could be repeated more than five times (Figure S1a).

The MCL of **1** was attributed to a typical crystalline-to-amorphous phase transition, which is triggered by mechanical grinding and reversed by heating. The differential scanning calorimetry (DSC) thermogram of crystalline **1** showed one endothermic peak, which represents the melting point of **1** (T_m = 173 °C; Figure 2d). Additionally, a broad exothermic peak that corresponds to the cold-crystallization transition (T_c = 92 °C) and a subsequent endothermic melting peak were observed in the DSC thermogram of the blue-green emissive ground **1**. PXRD analyses of the MCL of **1** revealed that the intensity of the diffraction pattern of crystalline **1** was significantly decreased after grinding and recovered after heating (Figure 2c).

A single crystal of **1** suitable for X-ray crystallography could not be obtained from various conditions using a variety of solvents. However, based on the observed emission wavelength and vibrational structure as well as the increased Φ_F and <τ> values upon grinding, the blue and blue-green emission of the crystalline

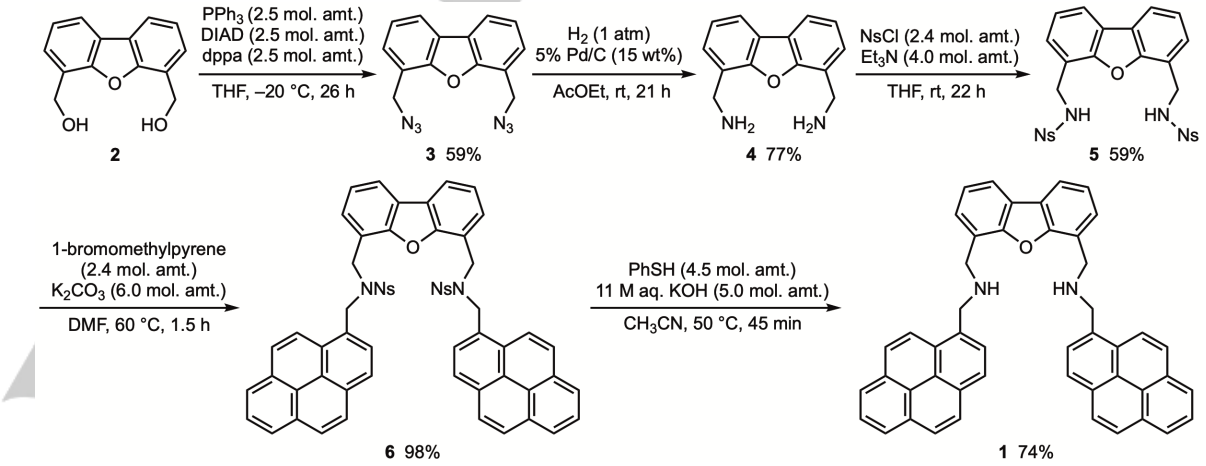

Scheme 1. Synthesis of dibenzofuran-based bis(1-pyrenylmethyl)diamine **1**.

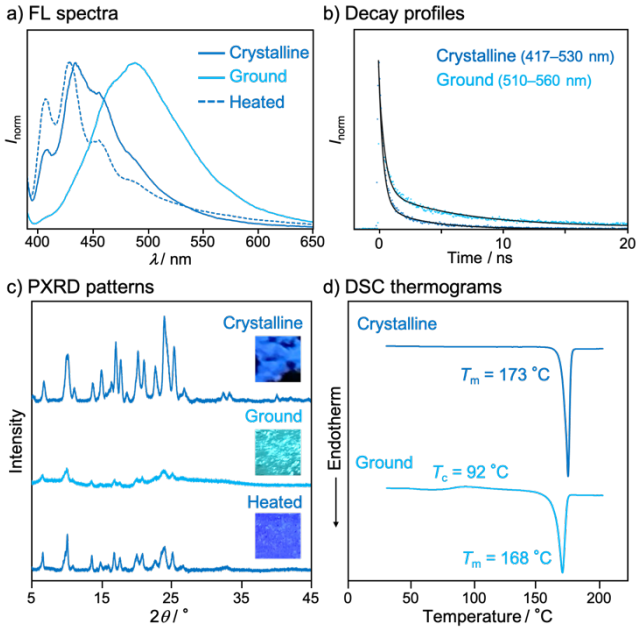

Figure 2. a) Fluorescence (FL) spectra of crystalline, ground, and heated samples of **1** (λ_{ex} = 365 nm). b) Fluorescence decay profiles of crystalline and ground **1** recorded at the single-particle level (λ_{ex} = 405 nm). Bandpass filters were used [blue dots: crystalline **1** (417–430 nm); light blue dots: ground **1** (510–560 nm). The black lines indicate multi-exponential curves fitted to the time profiles. c) Photographs under UV light (λ_{ex} = 365 nm) and PXRD patterns of crystalline, ground, and heated samples of **1**. d) DSC scans of crystalline and ground samples of **1**. T_m and T_c values are noted near the corresponding peaks.

and ground samples correspond to the monomer and excimer emission of the pyrenyl group.[10a,12]

Wide-range MCL of two-component dyes 1/DMQA, 1/FS, and 1/PTCDI

Two-component dyes were prepared using a 1:1 molar mixture of MCL compound **1** and typical commercially available organic luminescent dyes that do not change the emission color after amorphization by grinding (Figures S2 and S3). Equimolar mixtures of **1** and the appropriate luminescent dye in dichloromethane were evaporated under reduced pressure, and the residues were dried at 140 °C. The MCL properties of the as-prepared two-component dyes were examined via manual grinding with a spatula.

When *N*,*N*′-dimethylquinacridone (**DMQA**), fluorescein (**FS**), or 3,4,9,10-perylenetetracarboxylic diimide (**PTCDI**) were used as the acceptor dye, the MCL shifts of the resulting two-component mixtures were significantly larger than that of **1** (Figure 3a–c). For example, the two-component dye **1**/**DMQA** exhibited a bicolor MCL transition between violet (λ_{em} = 403 nm) and orange (λ_{em} = 617 nm) emission under UV light (λ_{ex} = 365 nm) in response to grinding and heating to 135 °C (Figures 3a and S5a). Notably, the shift in the maximum emission wavelength in this MCL process is greater than 200 nm ($\Delta\lambda_{em}$ = 214 nm). This MCL process is fully reversible at least five times (Figure S1b) and is independent of the evaporation rate and solvent used to prepare **1**/**DMQA** (Figure S4).

PXRD and DSC measurements suggested that the MCL of the two-component dye **1**/**DMQA** originates from phase transitions between segregated crystalline dyes and a mixed amorphous state. The PXRD pattern of violet-emissive **1**/**DMQA** showed intense diffraction peaks that corresponded to a superposition of those of **1** and **DMQA** (Figure 4a). The DSC thermogram of violet-emissive **1**/**DMQA** exhibited one endothermic peak at 171 °C (Figure 4b). This temperature was in good agreement with the melting point of **1**, although the mixture of solids often induces cryoscopy. As the melting point of **DMQA** (286 °C, decomp.) is above 200 °C, only the **1** fraction in **1**/**DMQA**

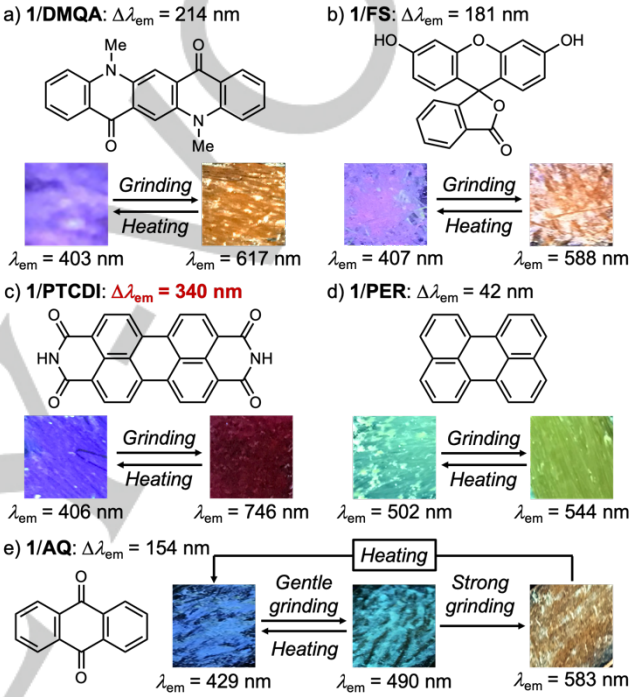

Figure 3. Chemical structures of the luminescent dyes and photographs of the MCL of the two-component organic dyes composed of **1** and the luminescent dyes. **DMQA**: *N*,*N*′-dimethylquinacridone; **FS**: fluorescein; **PTCDI**: 3,4,9,10-perylenetetracarboxylic diimide; **PER**: perylene; **AQ**: 9,10-anthraquinone.

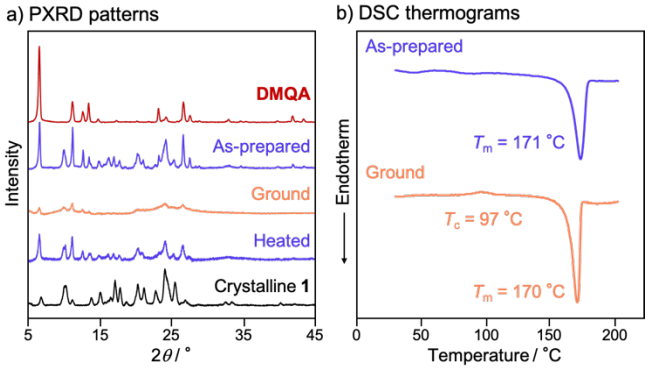

Figure 4. a) PXRD patterns of as-prepared, ground, and heated samples of **1**/**DMQA**. PXRD patterns of **DMQA** and crystalline **1** are shown for comparison. b) DSC thermograms of as-prepared and ground samples of **1**/**DMQA**. T_m and T_c values are noted near the corresponding peaks.

should be liquefied at this temperature. These results suggest that **1** and **DMQA** both exist as independent crystals in violet-emissive **1**/**DMQA**. In the orange-emissive ground **1**/**DMQA**, the intensity of the PXRD pattern decreased significantly (Figure 4a). The DSC thermogram of ground **1**/**DMQA** showed a broad exothermic cold-crystallization transition peak (T_c = 97 °C), followed by the endothermic melting point of **1** (T_m = 170 °C; Figure 4b). Accordingly, the orange-emissive samples of **1**/**DMQA** should exist in an amorphous state, and the segregated crystalline state was recovered from the amorphous state upon heating. After heating ground **1**/**DMQA** to 135 °C, the superimposed PXRD patterns of **1** and **DMQA** were again observed, which can confirm the formation of segregated crystals of **1** and **DMQA**. The regrinding of the heated sample afforded almost the same fluorescence spectrum, PXRD pattern, and DSC thermogram as those of the initial ground sample (Figures S8a, S9a, and S10a).

Similarly, the two-component mixture **1**/**FS** exhibited a wide-range MCL ($\Delta\lambda_{em}$ = 181 nm) transition between violet (λ_{em} = 407 nm) and orange (λ_{em} = 588 nm) emission (Figures 3b and S5b). Most remarkably, the emission wavelength of the two-component dye **1**/**PTCDI** bathochromically shifted by 340 nm from violet (λ_{em} = 406 nm, Φ_F = 0.02) to far-red (λ_{em} = 746 nm, Φ_F = <0.01) (Figures 3c and 5). DSC and PXRD measurements suggested that the MCL of **1**/**FS** and **1**/**PTCDI** is due to phase transitions between segregated crystals and the mixed amorphous state, as in the case of **1**/**DMQA** (Figures S6a, S6b, S7a, and S7b).[13]

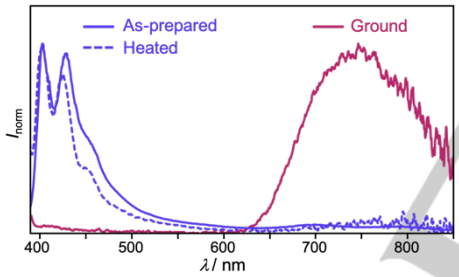

Figure 5. Fluorescence spectra showing the wide-range MCL of **1**/**PTCDI**.

Single-particle-level observations for the wide-range MCL of two-component dyes by fluorescence microscopy

The wide-range MCL of the two-component dye **1**/**PTCDI** was examined at the single-particle level using fluorescence microscopy, which provided further evidence that the two-component MCL originated from the transition between segregated crystals and a mixed amorphous state. In the single-particle-level observation of crystalline **1**/**PTCDI**, which exhibits violet emission in the bulk state, both strongly blue-emitting and weakly far-red-emitting regions were observed in the particle (Figure 6a and 6d).[14] The fluorescence spectra of the blue- and far-red-emissive regions were in good agreement with those of crystalline **1** and **PTCDI** recorded at the single-particle level using fluorescence microscopy (Figure S11a, S11b, and S11d). These results support the fact that **1** and **PTCDI** formed independent crystals in the two-component dye, which was suggested by the PXRD analyses. The observation of violet emission in the bulk state was attributed to the low emission intensity of the far-red luminescence from **PTCDI**. After grinding the segregated mixture, almost homogeneous far-red emission was observed via fluorescence microscopy (Figure 6b and 6d). The emission spectrum of the ground **1**/**PTCDI** was almost the same as that of ground **PTCDI** (Figure S11c and S11e). Accordingly, the far-red emission from **1**/**PTCDI** should not be attributed to the formation of an exciplex between the pyrenyl group of **1** and **PTCDI**. In the measurement of heated **1**/**PTCDI**, which was prepared by heating a ground sample to 155 °C for 20 min, segregated blue- and far-red-emissive regions were observed, along with small green-emissive regions (Figures 6c and S12a). The green emission was attributed to amorphous **1**, as the same emission spectrum was observed for green-emissive ground **1** (Figure S12b). The formation of the green-emissive regions can be explained by insufficient recrystallization of **1** upon heating. Despite the presence of small green-emissive regions, the emission color of heated **1**/**PTCDI** was violet in the bulk state. Most of the amorphous mixture of **1** and **PTCDI** should be crystallized independently after heating.

Detailed fluorescence lifetime measurements supported the possibility of FRET from **1** to **PTCDI** in ground **1**/**PTCDI** (Figure 6e and Table 1). Although **PTCDI** was virtually non-emissive in the bulk crystalline state due to the concentration quenching, far-red emission attributed to **PTCDI** was detected in the bulk sample of ground **1**/**PTCDI**. The increase in the emission intensity of ground **1**/**PTCDI** compared to that of ground **PTCDI** was attributed to energy transfer from **1** to **PTCDI** in the dispersed amorphous mixture. The fluorescence lifetimes of ground samples of **1** and **1**/**PTCDI** were measured using band-pass filters for the green (510–560 nm) and red (663–800 nm) regions. Green-emissive ground **1** exhibited two components (τ_1 = 0.40 ns; τ_2 = 4.67 ns) in

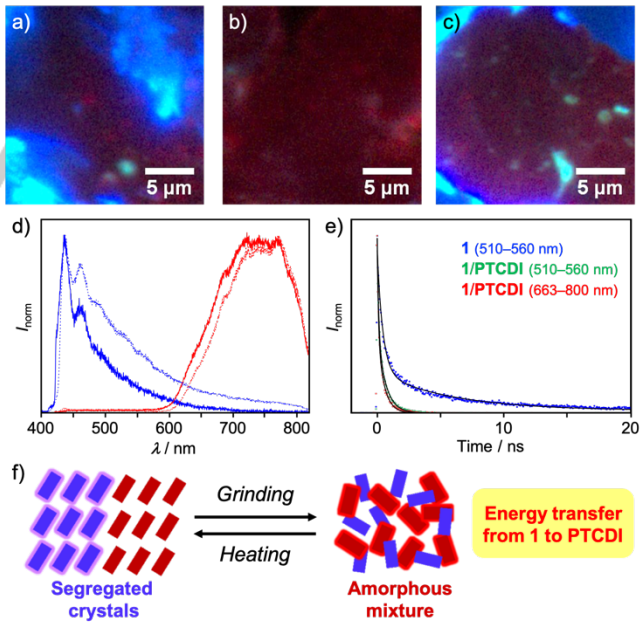

Figure 6. a–c) Photographs taken and edited with the same conditions, d) fluorescence spectra, and e) fluorescence decay profiles recorded at the single-particle level (λ_{ex} = 405 nm). a) As-prepared, b) ground, and c) heated samples of **1**/**PTCDI**. d) As-prepared (blue line), ground (red line), and heated (blue and red dotted lines) samples of **1**/**PTCDI**. e) Bandpass filters were used [blue and green dots: ground **1** and ground **1**/**PTCDI** (510–560 nm); red dots: ground **1**/**PTCDI** (663–800 nm)]. The black lines indicate multi-exponential curves fitted to the time profiles. f) Proposed mechanism for the wide-range MCL of **1**/**PTCDI**.

Table 1. Fluorescence decay times for ground samples of **1** and **1**/**PTCDI** in the green and red regions.

Sample	Region (nm)	τ_1 (ns)[a]	τ_2 (ns)[a]	$<\tau>$ (ns)[b]
Ground **1**	510–560	0.40 (0.67)	4.67 (0.24)	3.8
Ground **1**/**PTCDI**	510–560	0.11 (0.51)	0.65 (0.47)	0.57
	663–800	0.09 (0.53)	0.53 (0.46)	0.46

[a] The coefficient a_n of the component is shown in parentheses. [b] Intensity-weighted mean fluorescence lifetime. $<\tau> = (a_1\tau_1^2+a_2\tau_2^2)/(a_1\tau_1+a_2\tau_2)$.

the green region, and its $<\tau>$ was 3.8 ns. On the other hand, ground samples of **1**/**PTCDI** exhibited two components in both the green (τ_1 = 0.11 ns, τ_2 = 0.65 ns) and red (τ_1 = 0.09 ns, τ_2 = 0.53 ns) regions. Although no rise component was detected in the red region of ground **1**/**PTCDI**, the $<\tau>$ value of the red region ($<\tau>$ = 0.46 ns) was comparable to that in the green region ($<\tau>$ = 0.57 ns). Since a significant decrease in $<\tau>$ was observed in the green region of **1**/**PTCDI** ($<\tau>$ = 0.57 ns) compared to that of ground **1** ($<\tau>$ = 3.8 ns), a fast energy-transfer process from **1** to **PTCDI** should exist in the far-red-emissive amorphous state (Figure 6f). The FRET efficiency is calculated from the ratio of the $<\tau>$ values in the green region of ground **1**/**PTCDI** and ground **1** to be 0.85.

Single-particle-level observation of **1**/**DMQA** and **1**/**FS** revealed that these two-component dyes also form segregated crystals and homogeneous amorphous mixtures (Figure S13). In these cases, both intense blue emission and weak orange emission were found in the heated samples, and homogeneous orange emission was observed after grinding.

Bicolor MCL of two-component dye 1/PER

A two-component dye consisting of **1** and perylene (**PER**) exhibited bicolor MCL with a small shift ($\Delta\lambda_{em}$ = 42 nm; Figure 3d). The emission color of **1**/**PER** shifted bathochromically from blue-green (λ_{em} = 502 nm) to green (λ_{em} = 544 nm) upon grinding. Compared to the emission band of **1** (crystalline: λ_{em} = 433 nm; ground: λ_{em} = 487 nm), the blue-green emission of **1**/**PER** was shifted bathochromically. Additionally, green emission was detected from ground **1**/**PER** in the hypsochromic region relative to the emission of crystalline and ground **PER** (λ_{em} = ca. 595 nm; Figure S2d).

The relatively narrow-range MCL of **1**/**PER** compared to those of **1**/**DMQA**, **1**/**FS**, and **1**/**PTCDI** may be due to the lack of electron-accepting ability of **PER** and the formation of emissive mixtures by **1** and **PER**. Single-particle-level observation of **1**/**PER**, which exhibits blue-green emission in the bulk state, revealed almost homogeneous blue-green emission (Figure 7a and 7d). Similarly, apparently homogeneous green emission was observed for the samples after grinding (Figure 7b and 7d). A curve-fitting analysis of the fluorescence decay profiles indicated that both comprised two emissive components [blue-green: τ_1 = 1.42 ns (a_1 = 0.68), τ_2 = 4.18 ns (a_2 = 0.37); green: τ_1 = 0.40 ns (a_1 = 0.66), τ_2 = 5.72 ns (a_2 = 0.25)] (Figure 7e). On the other hand, a rise component was observed for the decay profile of the yellow emission from **PER** [τ_1 = 0.43 ns (a_1 = –0.27), τ_2 = 15.39 ns (a_2 = 1.00)], which indicates the formation of excimers (Figure 7c, 7d and 7e).[15] Based on the significantly longer τ value of **PER** compared to the τ_2 values of blue-green and green-emissive **1**/**PER**, the emission of **1**/**PER** does not include excimer emission from **PER**. Moreover, in the DSC thermogram of blue-green-emissive **1**/**PER** (Figure S7c), an endothermic peak was observed at 162 °C, which is 11 °C lower than the melting point of **1** (173 °C). Unlike for the other two-component dyes, depression of the melting point of **1** was caused by the formation of a mixture with **PER**. A PXRD analysis of the MCL of **1**/**PER** indicated typical crystal-to-amorphous transitions in response to mechanical and thermal stimuli (Figure S6c). However, the peaks attributed to the crystals of **PER** alone were not observed in the diffraction patterns of crystalline **1**/**PER**, indicating that once dissolved in dichloromethane, **PER** was not recrystallized independently in the presence of **1**.

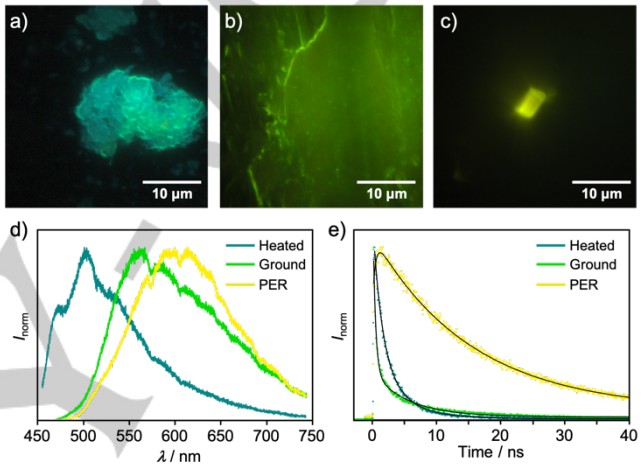

Figure 7. a–c) Photographs, d) fluorescence spectra, and e) fluorescence decay profiles recorded at the single-particle level (λ_{ex} = 405 nm). a) Blue-green emissive **1**/**PER**, b) green-emissive **1**/**PER**, and c) yellow-emissive **PER**. d and e) Blue-green emissive **1**/**PER** (blue-green line), green-emissive **1**/**PER** (green line), and yellow-emissive **PER** (yellow line). The black lines indicate multi-exponential curves fitted to the time profiles.

Two-step MCL of two-component dye 1/AQ

Uniquely, when the acceptor dye 9,10-anthraquinone (**AQ**) was mixed with **1**, the resulting two-component dye exhibited two-step MCL in response to mechanical stimuli of different intensity (Figure 3e). A 1:1 molar mixture of **1** and **AQ** in dichloromethane was evaporated and dried under heating. The resulting two-component dye **1**/**AQ** showed a blue emission band (λ_{em} = 429 nm) with vibrational structures (Figure 8a). Upon gently grinding **1**/**AQ** with a spatula, the intensity of the structured emission band at approximately 430 nm decreased significantly, and a broad emission band appeared (λ_{em} = 490 nm). The intensity of the gentle grinding was measured using a digital force gauge, which indicated a force of 5 N cm^{-2} (Table S2). Further strong grinding (11 N cm^{-2}) induced a significant bathochromic shift to give orange emission (λ_{em} = 583 nm) (Table S2). The original blue-emissive state was recovered from the orange-emissive state upon heating to 135 °C.

The DSC thermograms and PXRD patterns of **1**/**AQ** indicated that the segregated crystals of **1**/**AQ** initially change to a mixture of crystalline and amorphous phases upon gentle grinding and subsequently transition to a homogeneous amorphous state after

strong grinding (Figures S6d and S7d). The blue-emissive **1**/**AQ** showed an endothermic peak at 168 °C in its DSC thermogram and superimposed diffraction patterns of **1** and **AQ** in the PXRD analysis. Accordingly, we concluded that **1** and **AQ** form independent crystals in the blue-emissive **1**/**AQ**. An endothermic peak was observed at 164 °C for the blue-green-emissive **1**/**AQ** prepared by gentle grinding of the initial crystalline sample. Additionally, the intensity of the diffraction peaks in the PXRD pattern of gently ground **1**/**AQ** was weaker than that of crystalline **1**/**AQ**. Therefore, it is reasonable to assume that a fraction of the crystalline **1**/**AQ** was transformed into an amorphous state in response to gentle grinding. The amorphization of **1** and **AQ** by strong grinding was supported by the significantly decreased intensity of the diffraction peaks in the PXRD patterns of strongly ground **1**/**AQ**, which showed a broad exothermic T_c peak at approximately 88 °C in its DSC thermogram. The intensity of the diffraction patterns was recovered after heating ground **1**/**AQ** to 135 °C. The MCL transition between blue and blue-green-emissive states could be repeated by gentle grinding and heating to 90 °C, whereas the initial and orange-emissive states were reversible by strong grinding and heating to 135 °C (Figures S1d, S1e, S8c, S9c, S9d, S10c, and S10d).

Based on the single-particle level observations and fluorescence lifetimes measured using fluorescence microscopy, the origins of the blue, blue-green, and orange emission in the two-step MCL of **1**/**AQ** were assigned to emission from monomer **1**, excimer **1**, and charge-transfer (CT) complexes of **1** and **AQ**, respectively (Figure 8). Almost homogeneous emission was observed for all three states of **1**/**AQ**, even at the single-particle level (Figure 8a–e). The decay curves of the three states were well fitted by a double-exponential function, and a significant increase in <τ> was observed for the gently ground sample (Table 2; heated: 2.2 ns; gently ground: 5.7 ns; strongly ground: 2.5 ns). The bulk Φ_F of **1**/**AQ** also increased slightly after gentle grinding (heated: 0.05; gently ground: 0.06; strongly ground: 0.02). These results suggest that the emission-color change upon gentle grinding can be attributed to the MCL of **1** induced by the partial amorphization of **1**/**AQ** (Figure 8f). Although a PXRD analysis confirmed the crystallinity of gently ground **1**/**AQ** (Figure S6d), the blue-green emission should originate from the amorphous surface of the crystalline particles. In fact, the emission color of crystalline **1** changed to blue-green upon gentle grinding (5 N cm^{-2}), which corresponds to the intensity required for the first emission-color change of **1**/**AQ** (Table S2). Considering the low Φ_F of **AQ** in the solid state (Φ_F < 0.01), it is reasonable to conclude that only the MCL of **1** with a relatively high Φ_F (crystalline: 0.05; ground: 0.30) should be observed. On the other hand, the emission band of **1**/**AQ** induced by strong grinding (λ_{em} = 583 nm) was observed at considerably longer wavelength compared to those of crystalline and ground **AQ** (λ_{em} = ca. 525 nm; Figure S2e). As pyrene derivatives and anthraquinone derivatives are known to form CT complexes,[16] this bathochromic shift after strong grinding can be explained by emission from CT complexes between electron-donating **1** and electron-accepting **AQ** formed by the amorphization of **1** and **AQ** (Figure 8f).

An analysis of the absorption spectra confirmed that only **AQ** formed CT complexes with **1** after strong grinding. The absorption spectra of the non-MCL dyes were obtained by measuring their diffuse reflectance spectra. Significant overlap of the absorption band of the non-MCL dye with the emission band of ground **1** was observed for all the examined dyes except **AQ** (Figures 8g and S14a). Accordingly, energy transfer from **1** to the guest dyes

Table 2. Fluorescence decay times for heated, gently ground, and strongly ground samples of **1**/**AQ**.

Sample	λ_{em} (nm)	τ_1 (ns)[a]	τ_2 (ns)[a]	<τ> (ns)[b]
Heated	435	0.50 (0.81)	3.31 (0.19)	2.2
Gently ground	508	0.52 (0.71)	6.95 (0.22)	5.7
Strongly ground	599	0.31 (0.69)	3.10 (0.24)	2.5

[a] The coefficient a_n of the component is shown in parentheses. [b] Intensity-weighted mean fluorescence lifetime. $<\tau> = (a_1\tau_1^2+a_2\tau_2^2)/(a_1\tau_1+a_2\tau_2)$.

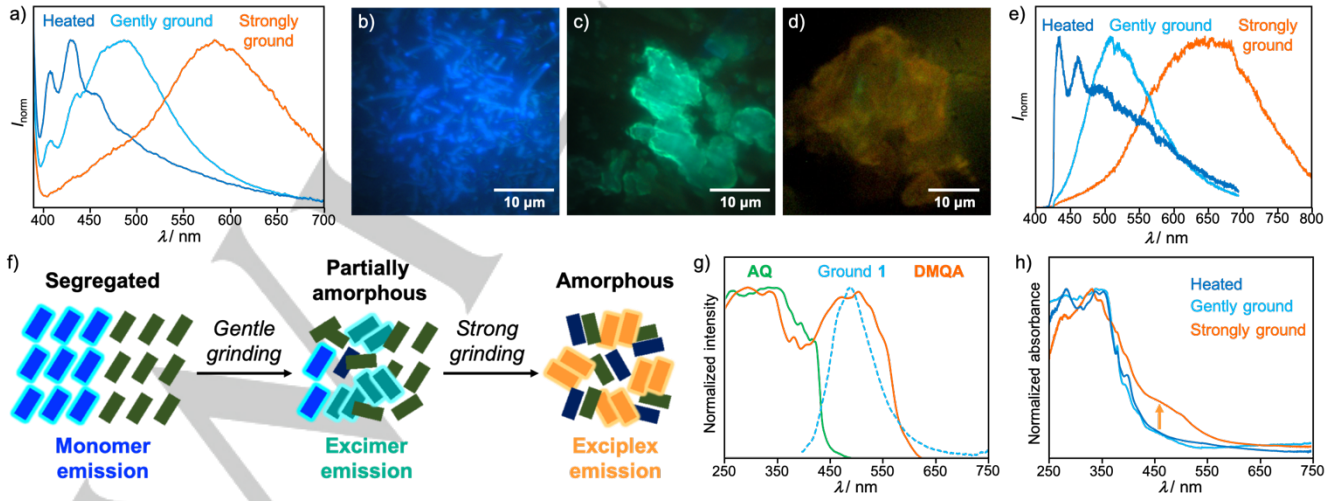

Figure 8. a) Fluorescence spectra of heated, gently ground, and strongly ground bulk samples of **1**/**AQ** (λ_{ex} = 365 nm). Photographs of b) heated, c) gently ground, and d) strongly ground samples of **1**/**AQ** at the single-particle level (λ_{ex} = 405 nm). e) Fluorescence spectra of heated, gently ground, and strongly ground samples of **1**/**AQ** at the single-particle level (λ_{ex} = 405 nm). f) Proposed mechanism for the two-step MCL of **1**/**AQ**. g) Fluorescence spectrum of ground **1** and solid-state absorption spectra of **DMQA** and **AQ**. h) Absorption spectra of heated, gently ground, and strongly ground samples of **1**/**AQ**.

(except in the case of **AQ**) should occur efficiently after grinding. In addition, in the case of **1**/**AQ**, the apparent color under ambient light clearly changed from pale-yellow to yellow after strong grinding (Figure S15). Absorption spectra of two-component dyes before and after grinding were measured using diffuse reflectance spectra (Figures 8h and S14b–e). The crystalline samples of the two-component dyes exhibited overlapped absorption spectra of those of **1** (Figure S14f) and the luminescent dyes (Figure S14a). The absorption spectra of the two-component dyes **1**/**DMQA**, **1**/**FS**, **1**/**PTCDI**, and **1**/**FS** were almost unchanged after grinding (Figure S14b–e). In sharp contrast, a new absorption band appeared at approximately 450 nm after grinding **1**/**AQ** strongly (Figures 8h and S16), which indicates the formation of CT complexes between the pyrenyl group of **1** and **AQ**.

Proposed mechanisms for the wide-range MCL and two-step MCL of two-component dyes

One of the reasons why two-component dyes of **1** with FRET acceptors (**DMQA**, **FS**, and **PTCDI**) do not exhibit two-step MCL could be rationalized as follows (Figure S17). After gentle grinding, a fraction of crystalline **1** and acceptor dyes changes to amorphous states. In this partially amorphous state, the energy transfer should occur from the excited state of amorphous **1** to both crystalline and partially amorphous acceptor dyes. Accordingly, blue-green excimer emission from amorphous **1** should be a minor component in the emission from gently ground samples of **1** with FRET acceptors.

The energy transfer and the formation of CT complexes in solution states were observed at different concentrations (10^{-5}~10^{-3} M for energy transfer and >10^{-3} M for CT formation; Figures S18–20). In a chloroform solution (**1** = 1.0×10^{-4} M), the intensity of excimer emission from **1** significantly decreased in the presence of an equimolar amount of **DMQA**, which should be attributed to the FRET from the long-lived excimer of the pyrenyl groups of **1** to **DMQA**.[17] The decrease in intensity was more pronounced at a higher concentration of the mixture of **1** and **DMQA** (**1** = 1.0×10^{-3} M, Figure S18). The emission maximum of **DMQA** shifted in the bathochromic direction at the high concentration probably due to the self-absorption of **DMQA**. Moreover, although **PTCDI** was not fully dissolved in DMF, a significant decrease in the emission intensity of **1** and the emission from aggregated **PTCDI** were observed for the suspension of **1** (5.0×10^{-5} M) with **PTCDI** (**1**/**PTCDI** = 1:1 to 1:3) in DMF (Figure S19). As shown in Table 1, the contribution of the FRET process in the solid state was supported by the decrease in the fluorescence lifetime at the excimer region (<τ>: ground **1**, 3.8 ns; ground **1**/**PTCDI**, 0.57 ns), although the radiative energy transfer by reabsorption may also occur in the solid state from the excimer emission of **1** to the FRET acceptors owing to the efficient overlaps between the excimer emission band of **1** and the absorption bands of the acceptor dyes.[18] In contrast, the CT band of **1** and **AQ** was not prominent in a chloroform solution of the 1:1 mixture of them even at a concentration of 5.0×10^{-3} M. A significant increase of the CT band was observed in the presence of 5 equivalents of **AQ** (**1**: 5.0×10^{-3} M; **AQ**: 2.5×10^{-2} M) (Figure S20).

The difficulties associated with forming CT complexes compared to those associated with energy transfer from **1** to the acceptor dyes can account for the origin of two-step MCL. FRET, which requires overlap between the emission spectrum of the donor and the absorption spectrum of the acceptor, typically occurs when the donor and acceptor dyes are separated by a distance of 10 to 100 Å.[19] In contrast, CT complexes are generally formed by donor and acceptor rings within the distance where the adjacent molecules can form mixed π orbitals (<5 Å).[20] Therefore, FRET from **1** to crystalline acceptor dyes should easily be occurred upon the partial amorphization of **1** by gentle grinding. On the other hand, CT complexes should not be formed between amorphous **1** and crystalline **AQ**, and a strong mechanical stimulus is required to form CT complexes of **1** and **AQ** by the sufficient amorphization of both **1** and **AQ**.

Conclusions

In conclusion, the MCL properties of dibenzofuran-based bis(1-pyrenylmethyl)diamine **1** were tuned by mixing **1** with a variety of non-MCL fluorophores. Most remarkably, wide-range MCL with a maximum emission wavelength shift of 340 nm was achieved using **PTCDI**. To the best of our knowledge, this is the first example of a two-component organic dye that exhibits an MCL shift of over 300 nm. Fluorescence microscopy, as well as PXRD and DSC analyses were applied to analyze the two-component dyes. The results revealed that the MCL of two-component dyes originates from the transition of segregated two-component crystals to a homogeneous amorphous state upon mechanical stimulation. The segregated crystals could easily be prepared and recovered by simply heating the two-component mixtures. The recovery of the segregated crystals should be facilitated by a small portion of unchanged crystalline phases of **1** and non-MCL fluorophores. In the cases of **DMQA**, **FS**, and **PTCDI**, FRET from **1** to the acceptor dye is promoted by the amorphization of **1** after grinding. This strategy can be expected to become a general method to control the MCL properties of various organic dyes other than **1**. Furthermore, the two-component dye of **1** and **AQ** showed a two-step emission-color change in response to mechanical stimuli of different intensity. A mechanism for this two-step MCL was proposed based on the stepwise formation of the excimer of pyrenyl groups in **1** upon gentle grinding followed by the formation of the exciplex between the pyrenyl group and **AQ** upon strong grinding. The inefficient energy transfer process from amorphous **1** to crystalline **AQ** should account for the observation of blue-green excimer emission from amorphous **1** in the gently ground state. The mechanical-stimulus-induced formation of CT complexes represents a promising method for rationally achieving multicolor MCL. Materials that exhibit MCL with a large wavelength shift or stepwise emission-color change without changing the excitation wavelength are expected to find a wide variety of potential applications in mechano-sensing technologies. The basic insights of this study should thus provide useful guidelines for the design of organic materials with specific MCL properties and further promote research into the practical applications of organic MCL dyes.

Acknowledgements

This work was partly supported by JSPS KAKENHI Grant Numbers 20K05645 within a Grant-in-Aid for Scientific Research

(C) as well as 18H04508, 18H04517, 20H04665, and 20H04673 within a Grant-in-Aid for Scientific Research on Innovative Areas ("Soft Crystals: Area No. 2903"). Part of this work was carried out by the joint research program No. R02019 of Molecular Photoscience Research Center, Kobe University. The authors are grateful to Ms. Masayo Ishikawa (Materials Analysis Suzukake-dai Center, Technical Department, Tokyo Institute of Technology) for FAB-HRMS analyses.

Keywords: dyes/pigments • luminescence • mechanochromism • photochemistry

[1] For recent reviews, see: a) S. Ito, *Chem. Lett.* **2021**, *50*, 649–660; b) M. Kato, H. Ito, M. Hasegawa, K. Ishii, *Chem. - Eur. J.* **2019**, *25*, 5105–5112; c) C. Wang, Z. Li, *Mater. Chem. Front.* **2017**, *1*, 2174–2194; d) Y. Sagara, S. Yamane, M. Mitani, C. Weder, T. Kato, *Adv. Mater.* **2016**, *28*, 1073–1095.

[2] For seminal examples of MCL materials, see: a) S. Yagai, S. Okamura, Y. Nakano, M. Yamauchi, K. Kishikawa, T. Karatsu, A. Kitamura, A. Ueno, D. Kuzuhara, H. Yamada, T. Seki, H. Ito, *Nat. Commun.* **2014**, *5*, 4013; b) K. Nagura, S. Saito, H. Yusa, H. Yamawaki, H. Fujihisa, H. Sato, Y. Shimoikeda, S. Yamaguchi, *J. Am. Chem. Soc.* **2013**, *135*, 10322–10325; c) H. Ito, M. Muromoto, S. Kurenuma, S. Ishizaka, N. Kitamura, H. Sato, T. Seki, *Nat. Commun.* **2013**, *4*, 2009; d) Y. Dong, B. Xu, J. Zhang, X. Tan, L. Wang, J. Chen, H. Lv, S. Wen, B. Li, L. Ye, B. Zou, W. Tian, *Angew. Chem. Int. Ed.* **2012**, *51*, 10782–10785; *Angew. Chem.* **2012**, *124*, 10940–10943; e) J. Wang, J. Mei, R. Hu, J. Z. Sun, A. Qin, B. Z. Tang, *J. Am. Chem. Soc.* **2012**, *134*, 9956–9966; f) B. Xu, Z. Chi, X. Zhang, H. Li, C. Chen, S. Liu, Y. Zhang, J. Xu, *Chem. Commun.* **2011**, *47*, 11080–11082; g) X. Luo, J. Li, C. Li, L. Heng, Y. Q. Dong, Z. Liu, Z. Bo, B. Z. Tang, *Adv. Mater.* **2011**, *23*, 3261–3265; h) G. Zhang, J. Lu, M. Sabat, C. L. Fraser, *J. Am. Chem. Soc.* **2010**, *132*, 2160–2162; i) S. J. Yoon, J. W. Chung, J. Gierschner, K. S. Kim, M. G. Choi, D. Kim, S. Y. Park, *J. Am. Chem. Soc.* **2010**, *132*, 13675–13683; j) S. Perruchas, X. F. L. Goff, S. Maron, I. Maurin, F. Guillen, A. Garcia, T. Gacoin, J. P. Boilot, *J. Am. Chem. Soc.* **2010**, *132*, 10967–10969; k) Y. Ooyama, Y. Kagawa, H. Fukuoka, G. Ito, Y. Harima, *Eur. J. Org. Chem.* **2009**, 5321–5326; l) H. Ito, T. Saito, N. Oshima, N. Kitamura, S. Ishizaka, Y. Hinatsu, M. Wakeshima, M. Kato, K. Tsuge, M. Sawamura, *J. Am. Chem. Soc.* **2008**, *130*, 10044–10045; m) Y. Sagara, T. Kato, *Angew. Chem. Int. Ed.* **2008**, *47*, 5175–5178; *Angew. Chem.* **2008**, *120*, 5253–5256; n) J. Kunzelman, M. Kinami, B. R. Crenshaw, J. D. Protasiewicz, C. Weder, *Adv. Mater.* **2008**, *20*, 119–122; o) Y. Sagara, T. Mutai, I. Yoshikawa, K. Araki, *J. Am. Chem. Soc.* **2007**, *129*, 1520–1521.

[3] Although the total number of organometallic MCL dyes is lower than that of organic MCL dyes, organometallic MCL dyes often exhibit distinct shifts of the emission bands. For organometallic MCL dyes that exhibit MCL shifts of over 100 nm, see: a) R. Kobayashi, T. Fujii, H. Imoto, K. Naka, *Eur. J. Inorg. Chem.* **2021**, 217–222; b) C.-Y. Lien, Y.-F. Hsu, Y.-H. Liu, S.-M. Peng, T. Shinmyozu, J.-S. Yang, *Inorg. Chem.* **2020**, *59*, 11584–11594; c) B. Hupp, J. Nitsch, T. Schmitt, R. Bertermann, K. Edkins, F. Hirsch, I. Fischer, M. Auth, A. Sperlich, A. Steffen, *Angew. Chem. Int. Ed.* **2018**, *57*, 13671–13675; *Angew. Chem.* **2018**, *130*, 13860–13864; d) M. Jin, T. Sumitani, H. Sato, T. Seki, H. Ito, *J. Am. Chem. Soc.* **2018**, *140*, 2875–2879; e) T. Seki, N. Tokodai, S. Omagari, T. Nakanishi, Y. Hasegawa, T. Iwasa, T. Taketsugu, H. Ito, *J. Am. Chem. Soc.* **2017**, *139*, 6514–6517; f) M. Jin, T. Seki, H. Ito, *Chem. Commun.* **2016**, *52*, 8083–8086; g) O. Toma, M. Allain, F. Meinardi, A. Forni, C. Botta, N. Mercier, *Angew. Chem. Int. Ed.* **2016**, *55*, 7998–8002; *Angew. Chem.* **2016**, *128*, 8130–8134; h) O. Toma, N. Mercier, C. Botta, *J. Mater. Chem. C* **2016**, *4*, 5940–5944; i) D. Genovese, A. Aliprandi, E. A. Prasetyanto, M. Mauro, M. Hirtz, H. Fuchs, Y. Fujita, H. Uji-I, S. Lebedkin, M. Kappes, L. De Cola, *Adv. Funct. Mater.* **2016**, *26*, 5271–5278; j) H. Ito, T. Saito, N. Oshima, N. Kitamura, S. Ishizaka, Y. Hinatsu, M. Wakeshima, M. Kato, K. Tsuge, M. Sawamura, *J. Am. Chem. Soc.* **2008**, *130*, 10044–10045.

[4] A limited number of organic MCL dyes exhibits MCL shifts of over 100 nm; for details, see: a) H. Yu, X. Song, N. Xie, J. Wang, C. Li, Y. Wang, *Adv. Funct. Mater.* **2020**, 2007511; b) W. Yang, Y. Yang, Y. Qiu, X. Cao, Z. Huang, S. Gong, C. Yang, *Mater. Chem. Front.* **2020**, *4*, 2047–2053; c) Y. Tsuchiya, K. Yamaguchi, Y. Miwa, S. Kutsumizu, M. Minoura, T. Murai, *Bull. Chem. Soc. Jpn.* **2020**, *93*, 927–935; d) Z. Xie, T. Su, E. Ubba, H. Deng, Z. Mao, T. Yu, T. Zheng, Y. Zhang, S. Liu, Z. Chi, *J. Mater. Chem. C* **2019**, *7*, 3300–3305; e) Y. Shen, P. Xue, J. Liu, J. Ding, J. Sun, R. Lu, *Dyes Pigm.* **2019**, *163*, 71–77; f) M. K. Panda, N. Ravi, P. Asha, A. P. Prakasham, *CrystEngComm* **2018**, *20*, 6046–6053; g) S. Cherumukkil, S. Ghosh, V. K. Praveen, A. Ajayaghosh, *Chem. Sci.* **2017**, *8*, 5644–5649; h) B. Xu, Y. Mu, Z. Mao, Z. Xie, H. Wu, Y. Zhang, C. Jin, Z. Chi, S. Liu, J. Xu, Y.-C. Wu, P.-Y. Lu, A. Lien, M. R. Bryce, *Chem. Sci.* **2016**, *7*, 2201–2206; i) M. Tanioka, S. Kamino, A. Muranaka, Y. Ooyama, H. Ota, Y. Shirasaki, J. Horigome, M. Ueda, M. Uchiyama, D. Sawada, S. Enomoto, *J. Am. Chem. Soc.* **2015**, *137*, 6436–6439; j) Z. Ma, M. Teng, Z. Wang, X. Jia, *Tetrahedron Lett.* **2013**, *54*, 6504–6506.

[5] a) S. Saotome, K. Suenaga, K. Tanaka, Y. Chujo, *Mater. Chem. Front.* **2020**, *4*, 1781–1788; b) S. Takahashi, S. Nagai, M. Asami, S. Ito, *Mater. Adv.* **2020**, *1*, 708–719; c) S. Nagai, M. Yamashita, T. Tachikawa, T. Ubukata, M. Asami, S. Ito, *J. Mater. Chem. C* **2019**, *7*, 4988–4998; d) C. Duan, Y. Zhou, G.-G. Shan, Y. Chen, W. Zhao, D. Yuan, L. Zeng, X. Huang, G. Niu, *J. Mater. Chem. C* **2019**, *7*, 3471–3478; e) A. Adak, T. Panda, A. Raveendran, K. S. Bejoymohandas, K. S. Asha, A. P. Prakasham, B. Mukhopadhyay, M. K. Panda, *ACS Omega* **2018**, *3*, 5291–5300; f) X. Wu, J. Guo, Y. Cao, J. Zhao, W. Jia, Y. Chen, D. Jia, *Chem. Sci.* **2018**, *9*, 5270–5277; g) Y. Zhou, L. Qian, M. Liu, X. Huang, Y. Wang, Y. Cheng, W. Gao, G. Wu, H. Wu, *J. Mater. Chem. C* **2017**, *5*, 9264–9272.

[6] a) Y. Li, Z. Ma, A. Li, W. Xu, Y. Wang, H. Jiang, K. Wang, Y. Zhao, X. Jia, *ACS Appl. Mater. Interfaces* **2017**, *9*, 8910–8918; b) Z. Ma, Z. Wang, Y. Li, S. Song, X. Jia, *Tetrahedron Lett.* **2016**, *57*, 5377–5380; c) Z. Ma, Y. Ji, Z. Wang, G. Kuang, X. Jia, *J. Mater. Chem. C* **2016**, *4*, 10914–10918; d) Z. Ma, Z. Wang, X. Meng, Z. Ma, Z. Xu, Y. Ma, X. Jia, *Angew. Chem. Int. Ed.* **2016**, *55*, 519–522; *Angew. Chem.* **2016**, *128*, 529–532.

[7] H.-J. Kim, D. R. Whang, J. Gierschner, C. H. Lee, S. Y. Park, *Angew. Chem. Int. Ed.* **2015**, *54*, 4330–4333; *Angew. Chem.* **2015**, *127*, 4404–4407.

[8] a) M. Ikeya, G. Katada, S. Ito, *Chem. Commun.* **2019**, *55*, 12296–12299; b) S. Ito, G. Katada, T. Taguchi, I. Kawamura, T. Ubukata, M. Asami, *CrystEngComm* **2019**, *21*, 53–59.

[9] Z. Wang, F. Yu, W. Chen, J. Wang, J. Liu, C. Yao, J. Zhao, H. Dong, W. Hu, Q. Zhang, *Angew. Chem. Int. Ed.* **2020**, *59*, 17580–17586; *Angew. Chem.* **2020**, *132*, 17733–17739.

[10] a) S. Ito, R. Sekine, M. Munakata, M. Asami, T. Tachikawa, D. Kaji, K. Mishima, Y. Imai, *ChemPhotoChem* **2021**, DOI: 10.1002/cptc.202100087; b) S. Ito, M. Okuno, M. Asami, *Org. Biomol. Chem.* **2018**, *16*, 213–222; c) S. Ito, K. Ikeda, S. Nakanishi, Y. Imai, M. Asami, *Chem. Commun.* **2017**, *53*, 6323–6326; d) S. Ito, K. Ikeda, M. Asami, *Chem. Lett.* **2016**, *45*, 1379–1381.

[11] D. Rosario-Amorin, E. N. Duesler, R. T. Paine, B. P. Hay, L. H. Delmau, S. D. Reilly, A. J. Gaunt, B. L. Scott, *Inorg. Chem.* **2012**, *51*, 6667–6681.

[12] a) A. Inoue, K. Yoshihara, T. Kasuya, S. Nagakura, *Bull. Chem. Soc. Jpn.* **1972**, *45*, 720–725; b) J. B. Birks, A. A. Kazzaz, T. A. King, *Proc. R. Soc. A* **1966**, *291*, 556–569.

[13] The MCL process of **1**/**PTCDI** could also be repeated more than five times (Figure S1c). The reground samples of **1**/**PTCDI** exhibited almost the same fluorescence spectrum, PXRD pattern, and DSC thermogram as those of initially ground **1**/**PTCDI** (Figures S8b, S9b, and S10b).

[14] As the excitation wavelength used for the fluorescence microscopy was 405 nm, the emission color of crystalline **1**/**PTCDI** was slightly different from that in the bulk state, which was excited at 365 nm.

[15] L. Ma, K. J. Tan, H. Jiang, C. Kloc, M.-E. Michel-Beyerle, G. G. Gurzadyan, *J. Phys. Chem. A* **2014**, *118*, 838–843.

[16] T. Doi, T. Sakakibara, H. Kashida, Y. Araki, T. Wada, H. Asanuma, *Chem. – Eur. J.* **2015**, *21*, 15974–15980.

[17] For examples of FRET from pyrene excimers to acceptor dyes, see: a) I. O. Aparin, O. V. Sergeeva, A. S. Mishin, E. V. Khaydukov, V. A. Korshun, T. S. Zatsepin, *Anal. Chem.* **2020**, *92*, 7028–7036; b) M. Taki, S.

Azeyanagi, K. Hayashi, S. Yamaguchi, *J. Mater. Chem. C* **2017**, *5*, 2142–2148; c) G. Wang, X. Chang, J. Peng, K. Liu, K. Zhao, C. Yu, Y. Fang, *Phys. Chem. Chem. Phys.* **2015**, *17*, 5441–5449.

[18] The fluorescence lifetime of the donor remains unchanged when the radiative energy transfer occurs. a) Y. Yuan, H. Zhu, Y. Nagaoka, R. Tan, A. H. Davis, W. Zheng, Q. Chen, *Front. Chem.* **2019**, *7*, 145; b) C. Li, X. Liu, J. Qiu, *Phys. Chem. Chem. Phys.* **2018**, *20*, 26513–26521.

[19] R. B. Sekar, A. Periasamy, *J. Cell Biol.* **2003**, *160*, 629–633.

[20] C. R. Martinez, B. L. Iverson, *Chem. Sci.* **2012**, *3*, 2191–2201.

Entry for the Table of Contents

Insert graphic for Table of Contents here.

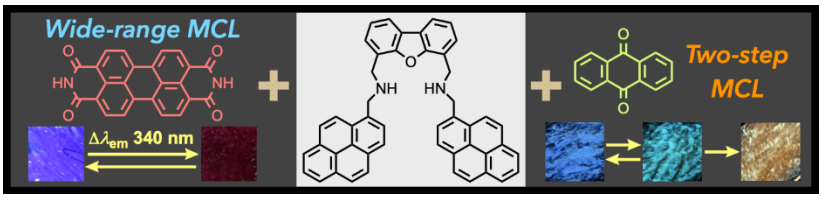

Insert text for Table of Contents here.

Control over the mechanochromic luminescence (MCL) of a dibenzofuran-based bis(1-pyrenylmethyl)diamine was achieved using a two-component donor–acceptor approach. Wide-range MCL with a solid-state emission wavelength shift of 340 nm and two-step MCL that can respond to mechanical stimuli of different intensity were realized for two-component mixtures composed of this diamine and a variety of non-MCL acceptor dyes.

Institute and/or researcher Twitter usernames: ((optional))